Journal of Chemical Crystallography (2026) 56:42
https://doi.org/10.1007/s10870-026-01101-9

ORIGINAL PAPER

Synthesis and Structural Characterization of $(H_2dabco)[Cu^{II}Br_4]$

Evgeny Goreshnik[1] · **Olha Panteleieva**[1,2]

Received: 23 January 2026 / Accepted: 3 June 2026

Abstract

The $(H_2dabco)[Cu^{II}Br_4]$ salt (dabco = 1,4-diazabicyclo[2.2.2]octane) was obtained and structurally characterized. The structure consists of isolated H_2dabco^{2+} cations and pseudo-tetrahedral $Cu^{II}Br_4^{2-}$ anions linked via N–H…Br hydrogen bonds along the 001 direction. Because the β-angle is very close to 90°, the unit cell parameters were examined over a temperature range from 290 to 90 K. No signs of a phase transition were observed. Strong distortion of the tetrahedral geometry of the $Cu^{II}Br_4^{2-}$ anion was discussed. The Hirshfeld surface was constructed and analyzed to better understand the nature of weak interactions.

Graphical Abstract

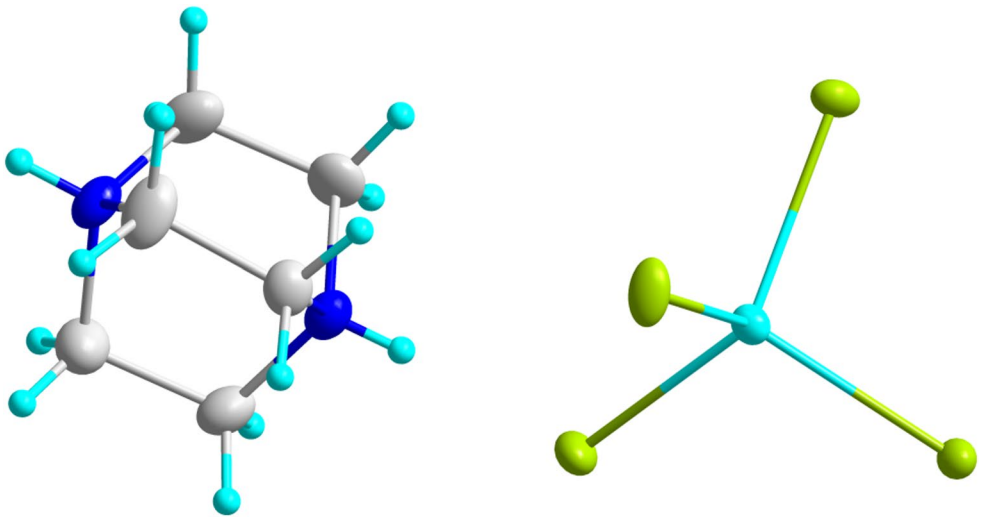

Keywords Copper · Bromide · 1,4-diazabicyclo[2.2.2]octane

✉ Evgeny Goreshnik
evgeny.goreshnik@ijs.si

[1] Department of Inorganic Chemistry and Technology, Jožef Stefan Institute, Jamova 39, 1000 Ljubljana, Slovenia

[2] Department of Chemistry and Chemical Engineering, University of Technology, av. Dmytra Yavornitskogo 19, Dnipro 49005, Ukraine

Published online: 29 June 2026

Introduction

Hybrid organic–inorganic compounds comprising mono- or di-protonated 1,4-diazabicyclo[2.2.2]octane (dabco) moieties and cupro-halide anions are notable for both the number and diversity of cupro-halide moieties. The CCDC contains 160 entries for such compounds, from that 56 records containe tetracoordinated copper center [1]. Copper chloride derivatives with dabco alone form isolated, one-dimensional, layered [2] and three-dimensional [3] cuprochloride moieties. Up to now five cuprobromide derivatives of dabco [4–9] have been structurally studied, while including all dabco derivatives expands this list to 41 entries in the CCDC. These salts are of interest not only from an academic perspective but also because of their useful properties, particularly luminescence and reversible thermochromism [5, 6, 9–13]. In addition, effective photodegradation of tetracycline in the presence of dabco derivative cuprobromide and cuproiodide has been reported [14].

In many cases, cupro-chlorides and cupro-bromides form isotypical compounds, such as $(H_2dabco)[Cu_3X_5]$ (X = Cl [2], Br [5]) or $(H_2dabco)[CuX_4]\cdot H_2O$ (X = Cl [15], Br [8]). However, a bromine analogue of $(H_2dabco)[CuCl_4]$ [15, 16] has not been reported. To address this, $(H_2dabco)[CuBr_4]$ was synthesized and characterized by single-crystal X-ray diffraction. The results are presented in this article.

Experimental Section

All chemicals were of commercial origin: $CuBr_2$ (Sigma Aldrich, 99%), HBr (Sigma Aldrich, 48% solution in water), 1,4-diazabicyclo[2.2.2]octane (Alfa Aesar, 98%), ethanol (Carlo Erba, p.a) were used without further purification.

Synthesis

Crystals of the new compound $(H_2dabco)[CuBr_4]$ were obtained by reacting 0.5–0.7 mmol of $CuBr_2$ with 0.1 mmol of dabco in a solution containing 18 ml of ethanol and 7 ml of 48% HBr, heated to 65–77 °C and stirred with a magnetic mixer for at least 5 h. Evaporation at elevated temperature produces a small amount of well-separated single crystals of compound **1** after about 3–4 days. Prolonged exposure to the mother liquor leads, after several days, to the transformation of crystals of compound **1** into the previously studied $(H_2dabco)CuBr_4\cdot H_2O$.

X–Ray Structure Determination

Preliminary data collection and structure solution yielded a suspicious monoclinic unit cell with a beta angle extremely close to 90 degrees. Due to concerns about the accuracy of the symmetry and to identify potential twinning, a multi-temperature experiment was conducted using CuKα radiation. Single-crystal X-ray data for compound **1** in the temperature range of 90–290 K were collected using graphite-monochromated CuKα radiation on a Gemini A diffractometer equipped with an Atlas CCD detector and a Cryostream 800 cooling device [17]. The data collection was performed up to 0.79 resolution limit, with 99.9% completeness and redundancy over 8. The data were processed using the CrysAlisPro program package. Despite the beta angle being very close to 90°, Rint values of 0.08 for the monoclinic setting and 0.54 for the orthorhombic setting (data measured at 150 K) clearly confirm the monoclinic symmetry. More than 90% reflections were indexed in the above monoclinic cell. Attempts to index the remaining fewer than 200 reflections as a second domain were unsuccessful. An analytical absorption correction was applied to the data set. The structure was solved using the dual-space algorithm in SHELXT [18], and refined using SHELXL-2014 [19], both implemented in the crystallographic software Olex [20]. Hydrogen atoms bound to carbon were placed in calculated positions (AFIX commands), with their thermal parameters set to 1.2Ueq of the corresponding carbon atoms. The positions of hydrogen atoms bound to nitrogen were located on difference Fourier maps and refined freely.

At the second stage, non-spherical atom refinement was performed using the NoSpherA2 procedure implemented in the Olex2 software [21]. Theoretical wavefunctions were calculated using ORCA 6.1 software [22], with the r2SCAN method and the def2-SVP basis set. Integration accuracy was set to Normal. Water was chosen as the solvation medium.

A multi-temperature experiment was performed with 20 K steps. The crystal was cooled at a rate of 30 K per hour. After reaching the desired temperature, a 15-min waiting period was used, then complete data were collected using the same strategy at each temperature.

The structural model at each temperature was examined using the PLATON/ADDSYM procedure. No indication of higher symmetry was observed. The CheckCIF report also does not contain any alerts regarding missed or higher symmetry. The PLATON/TwinRotMat procedure also did not indicate the presence of merohedral twinning. An analysis of geometric parameters $CuBr_4$ moieties from CCDC was performed by Mercury software [23]. Hirshfeld surface was built and analyzed using CrystalExplorer (version 21.5) software [24].

A summary of the crystallographic data and structure refinement is provided in Table 1. CCDC 2543564 (**1**) contains the supplementary crystallographic data for this paper. These data are available free of charge from the Cambridge

Table 1 Crystallographic data, details of data collection and structure refinement parameters

Formula	$C_6H_{14}Br_4CuN_2$	
M [g mol^{-1}]	497.37	
T [K]	150	
Crystal system	monoclinic	
Space group	$P2_1/c$	
a [Å]	9.2820(2)	
b [Å]	7.07097(16)	
c [Å]	19.2884(5)	
β [°]	90.073(2)	
V [Å^3]	1265.95(5)	
Z	4	
F(000)	932	
ρ_{calcd} [g cm^{-3}]	2.610	
Radiation, λ [Å]	CuKα, 1.54184	
μ [mm^{-1}]	16.925	
Absorption correction	Analytical numeric absorption correction using a multifaceted crystal model	
Crystal size, mm	0.50 × 0.37 × 0.20	
Crystal color and shape	Brown, block	
T_{max}, T_{min}	0.236, 0.039	
Rint	0.029	
Reflections all	23,758	
Independent	2642	
[I > 2σ(I)	2477	
	Independent atom model	NoSperA2
Goodness-of-fit on F^2	1.085	1.0651
Final R_1 [I > 2σ(I)]	0.0334	0.0324
Final R_1 (all data)	0.0371	0.0362
wR_2 [I > 2σ(I)]	0.0851	0.0818
wR_2 (all data)	0.0882	0.0848
Largest diff. peak and hole (e Å^{-3})	1.201, −1.245	0.8804, −0.9774

Crystallographic Data Centre via https://www.ccdc.cam.ac.uk/structures/.

Results and Discussion

NoSpherA2 vs IAM Refinement

The effects the IAM neglects include chemical bonding phenomena, electron lone pairs, weak interactions, and atom or molecular polarization [25]. These effects can only be described by applying a non-spherical treatment of the electron density of atoms in a crystal structure. As it is clear from the Table 1, the main improvement after NoSpherA2

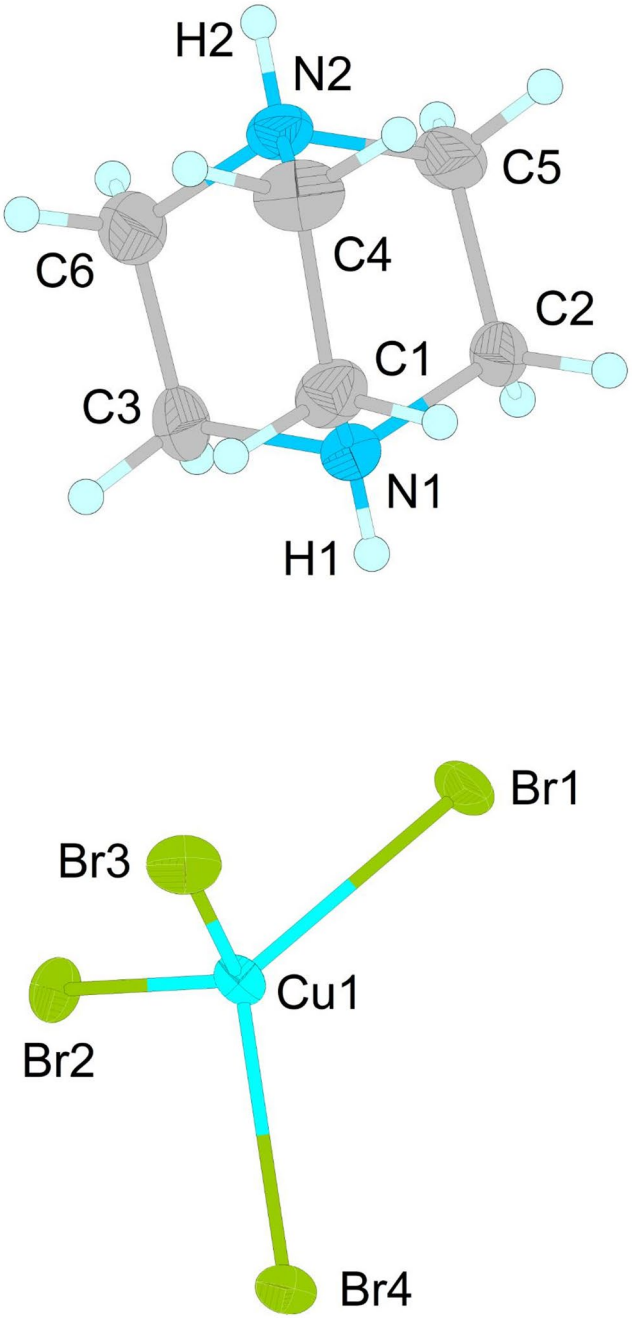

Fig. 1 Crystallographically independent part of crystal structure **1**. Thermal ellipsoids are drawn at 50% probability

Table 2 Comparison of unit cell parameters $(H_2dabco)[CuCl_4]$ (203 K, [16]) and $(H_2dabco)[CuBr_4]$ (200 K)

	Sp.gr	a (Å)	b (Å)	c (Å)	β(°)
$(H_2dabco)[CuCl_4]$	$P2_1/c$	8.997(2)	6.920(1)	18.804(4)	90.09(1)
$(H_2dabco)[CuBr_4]$	$P2_1/c$	9.2946(10)	7.0703(5)	19.2632(17)	90.103(7)

refinement in the case of $(H_2dabco)[CuBr_4]$ is noticeable decreasing of highest peaks of residual electron density.

Crystal Structure of 1

The compound $(H_2dabco)[CuBr_4]$ (**1**), consisting of $(H_2dabco)^{2+}$ di-cations and pseudo-tetrahedral $CuBr_4^{2-}$ anions (Fig. 1), is isotypic with the chloride analogue $(H_2dabco)[CuCl_4]$ (Table 2) [15, 16].

Three Cu–Br distances fall within a narrow range from 2.3619(6) to 2.3724(7) Å, while the Br4–Cu1 bond is slightly elongated at 2.4029(7) Å. In the closest related compound, $(H_2dabco)[CuBr_4]\cdot H_2O$, the Cu–Br distances are very similar: 2.3625(6)–2.4112(6) Å. The Br–Cu–Br angles span a broader range from 97.00(3) to 135.79(3) degrees (96.83(2)–133.95(3) degrees in $(H_2dabco)[CuBr_4]\cdot H_2O$). The peculiarities of the $CuBr_4$ geometry will be discussed later. Cations and anions are linked by N–H…Br hydrogen bonds. Each H(N) atom exhibits a different type of bonding: the H1 center forms an ordinary hydrogen bond, whereas the H2 atom participates in a bifurcated hydrogen bond with two bromide centers from the same anion (Table 3, Fig. 2).

Table 3 Hydrogen-bond geometry (Å, °) in the structure of compound **1**

D–H···*A*	*D*–H	H···*A*	*D*···*A*	*D*–H···*A*
N1–H1···Br1	0.79 (6)	2.67 (6)	3.275 (4)	135 (5)
N2–H2···Br2^{i}	0.84 (6)	2.76 (6)	3.346 (3)	128 (4)
N2–H2···Br4^{i}	0.84 (6)	2.70 (6)	3.417 (4)	144 (4)
C1–H1B···Br2^{ii}	1.11	2.78	3.684(4)	138
C2–H2A···Br3^{iii}	1.11	2.89	3.754(4)	135

Symmetry code: (i) x, −y+1/2, z−1/2, (ii) -x+1, -y+1, -z+1; (iii) x, y-1, z

These hydrogen bonds connect cations and anions into slightly wavy chains. Weak C–H…Br hydrogen bonds (H…Br 2.78–2.89 Å) further associate these chains.

Two peculiarities of the crystal structure attracted our attention. First, the monoclinic angle, which is very close to 90°, prompted us to investigate this structure at different temperatures to identify any possible phase transition. Surprisingly, the monoclinic symmetry remains unchanged over a rather wide temperature range–from room temperature to 90 K (Table 4). The data at each temperature were processed and carefully examined for the absence of reflections splitting, amount of non-indexed reflections, Rint

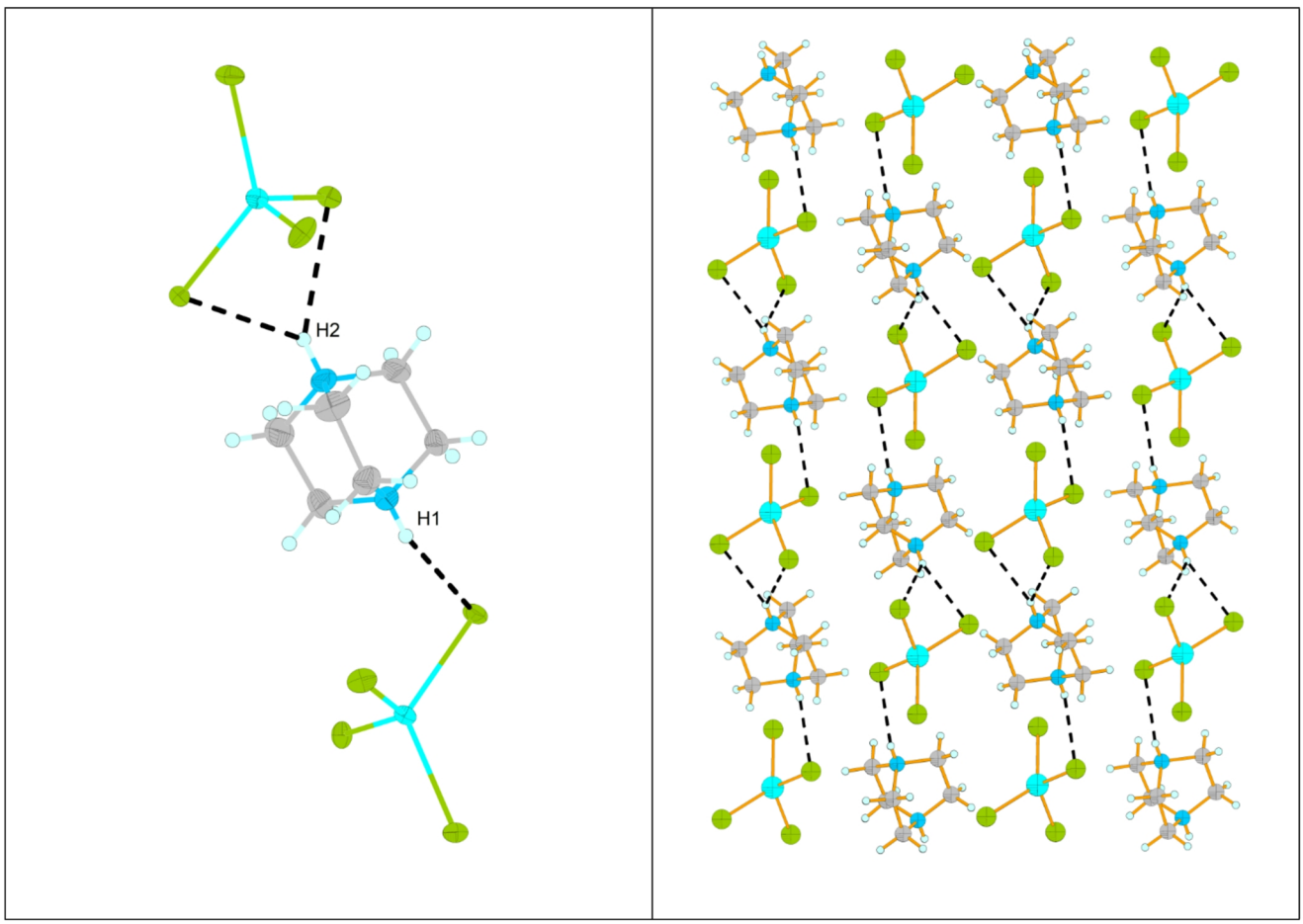

Fig. 2 Hydrogen bonds scheme (left) and packing (view along 010) of crystal structure **1**

Table 4 Unit cell parameters of compound **1** at different temperatures

T, K	*a* [Å]	b [Å]	c [Å]	β [°]	*V* [Å^3]
240	9.3184(10)	7.0829(9)	19.284(2)	90.087(9)	1272.8(3)
220	9.3057(10)	7.0761(9)	19.275(2)	90.096(9)	1269.2(3)
200	9.2946(10)	7.0703(5)	19.2632(17)	90.103(7)	1265.71(18)
180	9.2856(10)	7.0644(9)	19.262(2)	90.093(9)	1263.6(3)
160	9.2749(9)	7.0557(8)	19.255(2)	90.092(9)	1260.1(2)
140	9.2654(9)	7.0480(8)	19.249(2)	90.093(8)	1257.0(2)
120	9.2624(11)	7.0401(9)	19.262(2)	90.047(10)	1256.0(3)
100	9.2474(9)	7.0347(8)	19.244(2)	90.099(8)	1251.9(2)
90	9.2464(9)	7.0333(8)	19.248(2)	90.095(8)	1251.7(2)

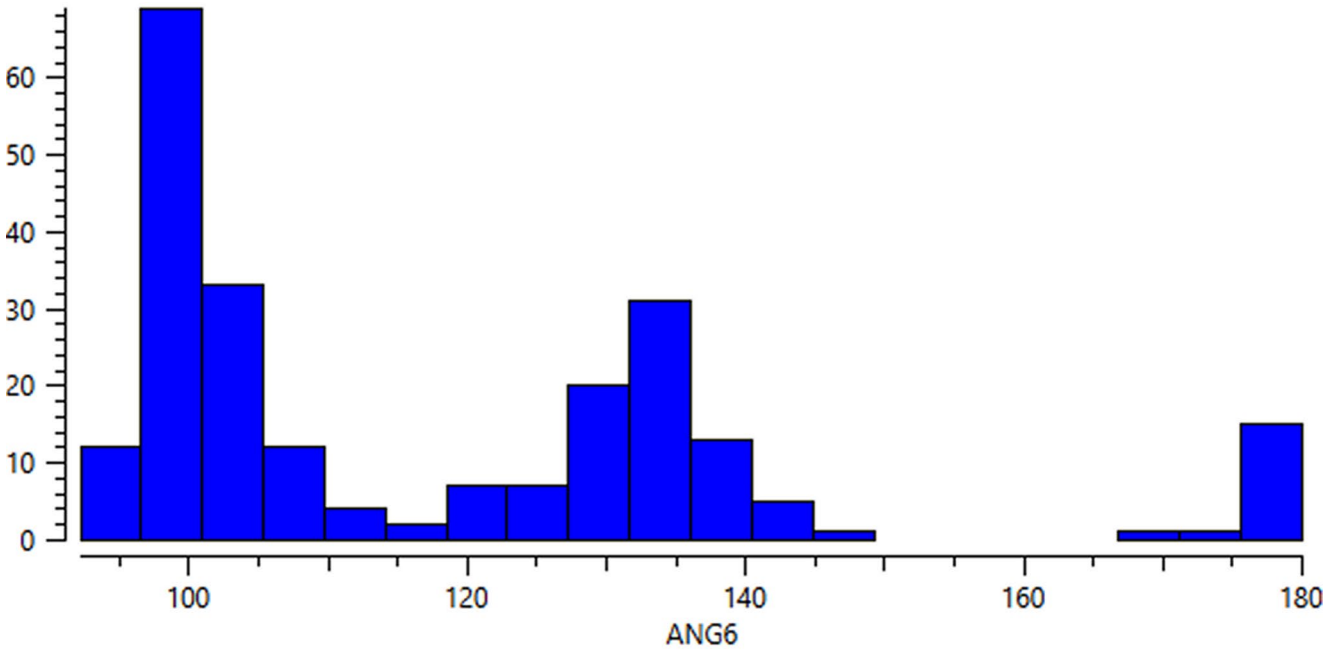

Fig. 3 Distribution of Br–Cu–Br angles in known $CuBr_4$ moieties

values, R- and GOOF values. Decreasing the temperature results in a monotonic contraction of each axis of the unit cell, while the beta angle remains unchanged within standard uncertainty. The linear expansion coefficients in the 100 and 010 directions are similar (5.17×10^{-5} K^{-1} and 4.69×10^{-5} K^{-1}, respectively), whereas the value for the 001 direction, 1.25×10^{-5} K^{-1}, is noticeably smaller. This difference is likely related to the shortest Br…Br distances of 3.88 Å (slightly longer than the sum of bromine van der Waals radii), which roughly coincide with the 001 direction. Thus, the thermal contraction of compound **1** is anisotropic.

Another unusual feature observed in compound **1** and related structures is the pronounced tetrahedral distortion of the CuX_4 coordination polyhedron. The τ4 parameter value of 0.76 indicates a significantly distorted tetrahedral environment (a value of 1.00 corresponds to a perfect tetrahedral geometry, while 0 corresponds to a perfect square-planar geometry) [26]. This value changes imperceptibly as the temperature decreases. Corresponding value observed in $(H_2dabco)[CuBr_4]\cdot H_2O$ salt is 0.68. Previously described $[H_2dabco][CuCl_4]$ and $[H_2dabco][CuCl_4]\cdot H_2O$ salts also contain pseudo-tetrahedral $CuCl_4^{2-}$ anions with τ4 parameter values of 0.74 and 0.66 respectively [15]. It should be noted that all known $(H_2dabco)^{2+}$ cupro(II) halides exhibit similar tetrahedral distortion of the CuX_4 anion. The CCDC contains 215 entries with $CuBr_4$ moieties [1]. A histogram of Br–Cu–Br angles (Fig. 3) in these anions shows a wide distribution, with two statistical maxima at 100 and 133 degrees respectively.

Alternative parameter for description of tetrahedral unit distortion is a value of dihedral angle between Br1–Cu–Br2 and Br3–Cu–Br4 planes. This parameter, being 90° for ideal tetrahedral $CuBr_4$ geometry, decreases with tetrahedron flattening. In the case of compound **1** respective value is 72.3^0. In earlier described $[H_2dabco][CuCl_4]$ and $[H_2dabco][CuCl_4]\cdot H_2O$ salts these parameters are 67.83 and 61.61

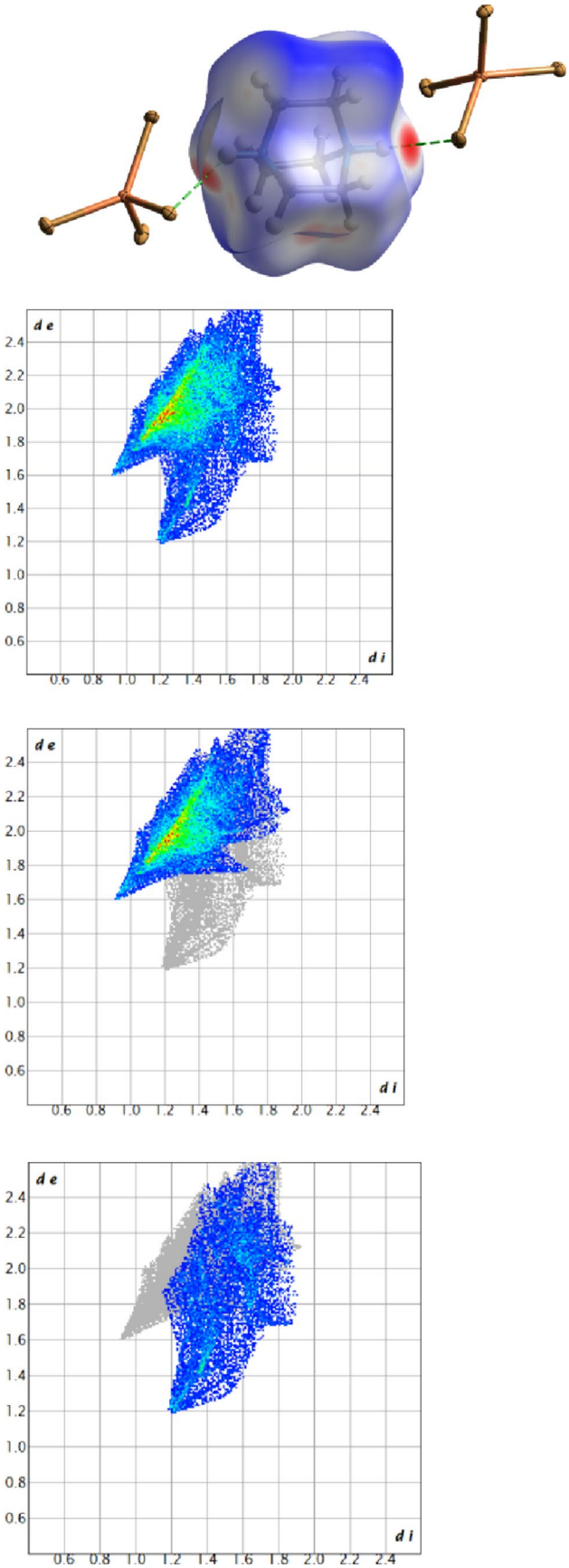

Fig. 4 Hirshfeld surface for $(H_2dabco)[CuBr_4]_2$ fragment mapped with d norm over the range -0.65 to 1.7, as well as fingerprint plots for molecules resolved into H…H and H…Br interactions

respectively. Another parameter of tetrahedral geometry distortion is the Bauer index. The angular Δθ parameter, calculated using the equation $\Delta\theta = \sqrt{\frac{1}{6}\sum_{i=1}^{6}(i-109.47)^2}$ (θ_i–all six Br–Cu–Br angles within $CuBr_4$ moiety) of 12.02 (0 for ideal tetrahedral geometry, 43.7 for square-planar geometry) indicates also strong flattening of $CuBr_4$ polyhedron. A highly flattened geometry was observed, for example, in the crystal structure of $[C_5H_7N_2]_2[CuBr_4]$ [27]. It was assumed that strong hydrogen bonds involving the bromine centers decrease the charge of the bromide ions and favor the flattened geometry of the $CuBr_4^{2-}$ anion [28]. Another (indirect) confirmation of this assumption is the regular tetrahedral geometry of the $CuBr_4^{2-}$ anion in $[(C_2H_5)_4N]_2[CuBr_4]$ salt, where the possibility of hydrogen bond formation is absent [29]. As shown above, in both monohydrate salts $(H_2dabco)[CuCl_4]\cdot H_2O$ and $(H_2dabco)[CuBr_4]\cdot H_2O$ with more opportunities for hydrogen bond formation the τ4 parameter values are noticeably lower than those in $(H_2dabco)[CuCl_4]$ and $(H_2dabco)[CuBr_4]$, respectively. On the other hand, the Jahn–Teller effect was cited as the reason for the distorted anion geometry in $(DAP\text{-}H_2)[CuBr_4]$ (DAP = hexahydrodiazepine ($C_5H_{14}N_2$)) which contains discrete $CuBr_4$ tetrahedra [30]. Probably, the presence of hydrogen bonds has stronger influence on coordination polyhedron distortion than Jahn–Teller effect.

To analize intermolecular interactions, the Hirshfeld surface was constructed for the $[H_2dabco][CuBr_4]_2$ fragment in **1**. Whole di-cation and two counter-ions were chosen to show complete picture of interactions around $[H_2dabco]$ moiety. The most significant N–H…Br interactions between cations and anions appear as red areas on the Hirshfeld surface plot (Fig. 4). Fingerprint plots were generated to show the intermolecular surface bond distances. The main contributions to the surface area are from H…Br (65.5%) and H…H (30.3%) contacts.

Conclusions

The new $(H_2dabco)[CuBr_4]$ salt was synthesized and structurally studied. Although the beta angle is very close to 90°, no signs of a phase transition were observed in the temperature range from 290 to 90 K. Similar to other H_2dabco cupro-halides, the $Cu^{II}Br_4^{2-}$ anion exhibits a well-pronounced tetrahedral distortion.

Acknowledgements Authors gratefully acknowledge the Slovenian Research Agency (ARRS) for the financial support of the present study within the research program P1-0045 Inorganic Chemistry and Technology. O.P. acknowledges the financial support from Erasmus+ program.

Author Contributions Conceptualisation—E.G., synthetic work—O.P., X-ray diffraction experiment —E.G., manuscript preparation—E.G. and O.P.

Funding The Slovenian Research and Innovation Agency, P1-0045, Erasmus+, European Union.

Data Availability Crystallographic data are available free of charge from the Cambridge Crystallographic Data Centre via https://www.ccdc.cam.ac.uk/structures/.

Declarations

Competing interests The authors declare no competing interests.

References

1. Groom CR, Bruno IJ, Lightfoot MP, Ward SC (2016) The Cambridge structural database. Acta Crystallogr B Struct Sci Cryst Eng Mater 72:171–179. https://doi.org/10.1107/S2052520616003954
2. Goreshnik E (2021) Influence of the synthetic conditions on a formation of 1-D, 2-D and 3-D copper–chloride coordination polymers. CrystEngComm 23:7171–7178. https://doi.org/10.1039/D1CE01048D
3. Williams ER, Weller MT (2013) Hydrothermal synthesis and structural characterisation of $[H_2DABCO]_3[Cu_{16}Cl_{22}]$: a new copper(I) chloride framework. CrystEngComm 15:31–33. https://doi.org/10.1039/C2CE26068A
4. Vakulka A, Goreshnik E (2018) Copper(I) bromide and chloride complexes with urotropine and triethylenediamine: synthesis, crystal structure, and Raman characterization. J Coord Chem 71:2426–2440. https://doi.org/10.1080/00958972.2018.1481210
5. Yue CY, Lin N, Gao L, Jin YX, Liu ZY, Cao YY, Han SS, Lian XK, Hu B, Lei XW (2019) Organic cation directed one-dimensional cuprous halide compounds: syntheses, crystal structures and photoluminescence properties. Dalton Trans 48:10151–10159. https://doi.org/10.1039/C9DT01460H
6. Maderlehner S, Leitl MJ, Yersin H, Pfitzner A (2015) Halocuprate(I) zigzag chain structures with N-methylated DABCO cations – bright metal-centered luminescence and thermally activated color shifts. Dalton Trans 44:19305–19313. https://doi.org/10.1039/C5DT02709H
7. Zhang XM, Hou JJ, Guo CH, Li CF (2015) A new class of cuprous bromide cluster-based hybrid materials: direct observation of the stepwise replacement of hydrogen bonds by coordination bonds. Inorg Chem 54:554–559. https://doi.org/10.1021/ic5024168
8. Zhang Y, Wang B (2011) 1,4-Diazoniabicyclo[2.2.2]octane tetrabromidocuprate(II) monohydrate. Acta Crystallogr E Struct Rep Online 67:m371. https://doi.org/10.1107/S1600536811005289
9. Panda DP, Swain D, Sundaresan A (2022) Photophysical and magnetic properties in zero-dimensional $(H_2DABCO)MX_4{\cdot}nH_2O$ (M = Mn and Cu; X = Cl and Br; n = 0, 1, and 4). J Phys Chem C 126:13291–13299. https://doi.org/10.1021/acs.jpcc.2c03481
10. Jing CQ, Wu JH, Cao YY, Che HX, Zhao XM, Yue M, Liao YY, Yue CY, Lei XW (2020) A three-dimensional cuprous lead bromide framework with highly efficient and stable thermochromic luminescence properties. Chem Commun 56:5925. https://doi.org/10.1039/D0CC01779E
11. Xin B, Sang J, Gao Y, Li G, Shi Z, Feng S (2018) A pillared-layered copper(I) halide-based metal–organic framework exhibiting dual emission, and piezochromic and thermochromic properties with a large temperature-dependent emission red-shift. RSC Adv 8:1973–1978. https://doi.org/10.1039/C7RA11950J
12. Zeng G, Xing S, Han X, Xin B, Yang Y, Wang X, Li G, Shi Z, Feng S (2015) Reversible photoluminescence switching behavior and luminescence thermochromism of copper(I) halide cluster coordination polymers. RSC Adv 5:40792–40797. https://doi.org/10.1039/C5RA05157F
13. Wan M, Chen HR, Wang YN, Shi K, Liu JY, Li ZM, Ye SY, Li JY, Chen LZ (2022) Reversible thermochromism to tune the bandgap of organic–inorganic hybrid materials. Mater Chem Front 6:3094–3101. https://doi.org/10.1039/D2QM00696K
14. Wang X, Zhu G, Wang C, Niu Y (2021) Effective degradation of tetracycline by organic-inorganic hybrid materials induced by triethylenediamine. Environ Res 198:111253. https://doi.org/10.1016/j.envres.2021.111253
15. Wei M, Willett RD (2002) A comparison of the crystal structures of $(dabcoH_2)CuCl_4$ and $(dabcoH_2)CuCl_4{\cdot}H_2O$. J Chem Crystallogr 32:439–445. https://doi.org/10.1023/A:1021188525007
16. Brammer L, Swearingen JK, Bruton EA, Sherwood P (2002) Hydrogen bonding and perhalometallate ions: a supramolecular synthetic strategy for new inorganic materials. Proc Natl Acad Sci U S A 99:4956. https://doi.org/10.1073/pnas.072623399
17. CrysAlisPro, Agilent Technologies, Version 1.171.37.31 (release 14–01–2014 CrysAlis171 .NET).
18. Sheldrick GM (2015) SHELXT – integrated space-group and crystal-structure determination. Acta Crystallogr A Found Adv 71:3–8. https://doi.org/10.1107/S2053273314026370
19. Sheldrick GM (2015) Crystal structure refinement with SHELXL. Acta Cryst C71:3–8. https://doi.org/10.1107/S2053229614024218
20. Dolomanov OV, Bourhis LJ, Gildea RJ, Howard JAK, Puschmann H (2009) OLEX2: a complete structure solution, refinement and analysis program. J Appl Cryst 42:339–341. https://doi.org/10.1107/S0021889808042726
21. Kleemiss F, Dolomanov OV, Bodensteiner M, Peyerimhoff N, Midgley L, Bourhis LJ, Genoni A, Malaspina LA, Jayatilaka D, Spencer JL, White F, Grundkötter-Stock B, Steinhauer B, Lentz D, Puschmann H, Grabowsky S (2021) Accurate crystal structures and chemical properties from NoSpherA2. Chem Sci 12:1675–1692. https://doi.org/10.1039/D0SC05526C
22. Neese F (2012) The ORCA program system. WIREs Comput Mol Sci 2:73–78. https://doi.org/10.1002/wcms.81
23. Macrae CF, Sovago I, Cottrell SJ, Galek PTA, McCabe P, Pidcock E, Platings M, Shields GP, Stevens JS, Towler M, Wood PA (2020) Mercury 4.0: from visualization to analysis, design and

prediction. J Appl Cryst 53:226–235. https://doi.org/10.1107/S1600576719014092
24. Spackman PR, Turner MJ, McKinnon JJ, Wolff SK, Grimwood DJ, Jayatilaka D, Spackman MA (2021) CrystalExplorer: a program for Hirshfeld surface analysis, visualization and quantitative analysis of molecular crystals. J Appl Crystallogr 54(3):1006–1011. https://doi.org/10.1107/S1600576721002910
25. Brüx D, Meurer F, Kleemiss F (2025) Benchmarking crystal structure refinement: a systematic study on Hirshfeld atom refinement. Struct Dyn 12:054101. https://doi.org/10.1063/4.0000774
26. Yang L, Powell DR, Houser RP (2007) Structural variation in copper(i) complexes with pyridylmethylamide ligands: structural analysis with a new four-coordinate geometry index, τ4. Dalton Trans. https://doi.org/10.1039/B617136B
27. Luque A, Sertucha J, Lezama L, Rojo T, Rom P (1997) Synthesis, characterisation and crystal structure of 2-aminopyridinium (2-amino-5-bromopyridine)tribromocuprate(II) and bis(2-aminopyridinium) tetrabromocuprate(II). J Chem Soc Dalton Trans. https://doi.org/10.1039/a606429i
28. Pelikán P, Liska M (1984) MO study of Td-D4h equilibrium in complexes of transition metals. II. Equilibrium in tetrafluoro and tetrabromo complexes of atoms of the first transition row. Collect Czech Chem Commun 49:2837. https://doi.org/10.1135/cccc19842837
29. Starova GL, Skripkin MY, Gusev IM (2010) Structure of complex bromides crystallizing in MBr_2-NEt_4Br-H_2O systems (M = Cd, Cu, Co) at 25°C. Russ J Gen Chem 80:1236–1241. https://doi.org/10.1134/S1070363210070030
30. Bourwina M, Msalmi R, Walha S, Turnbull M, Roisnel T, Guesmi A, Houas A, Ben Hamadi N, Naïli H (2023) Crystal chemistry, optic and magnetic characterizations of a new copper based material templated by hexahydrodiazepine. ACS Omega 8:15075–15082. https://doi.org/10.1021/acsomega.2c08035